

See discussions, stats, and author profiles for this publication at: <https://www.researchgate.net/publication/322589458>

# A general method to filter out defective spatial observations from yield mapping datasets

Article in *Precision Agriculture* · January 2018

DOI: 10.1007/s11119-017-9555-0

---

CITATIONS

0

---

READS

88

6 authors, including:



**Corentin Leroux**

Montpellier SupAgro

5 PUBLICATIONS 4 CITATIONS

SEE PROFILE



**Hazaël Jones**

Montpellier SupAgro

41 PUBLICATIONS 141 CITATIONS

SEE PROFILE



**Bruno Tisseyre**

Montpellier SupAgro

97 PUBLICATIONS 737 CITATIONS

SEE PROFILE

Some of the authors of this publication are also working on these related projects:



Pilotype [View project](#)



Pre-processing and zoning yield monitor data : Towards a variable rate nutrient balance [View project](#)

All content following this page was uploaded by [Corentin Leroux](#) on 22 January 2018.

The user has requested enhancement of the downloaded file.

# 1 A general method to filter out defective spatial observations from yield 2 mapping datasets

3 Leroux, Corentin (1-2), Jones, Hazaël (2), Clenet, Anthony (1), Dreux, Benoit (3), Becu, Maxime (3), Tisseyre,  
4 Bruno (2)

5  
6 (1) SMAG, Montpellier, France  
7 (2) UMR ITAP, Montpellier SupAgro, Irstea, France  
8 (3) DEFISOL, Evreux, France  
9 [cleroux@smag-group.com](mailto:cleroux@smag-group.com)

10

## 11 Abstract

12 Yield maps are recognized as a valuable tool with regard to managing upcoming crop production but can contain  
13 a large amount of defective data that might result in misleading decisions. These anomalies must be removed  
14 before further processing to ensure the quality of future decisions. This paper proposes a new holistic methodology  
15 to filter out defective observations likely to be present in yield datasets. The notion of spatial neighbourhood has  
16 been refined to embrace the specific characteristics of such on-the-go vehicle based datasets. Observations are  
17 compared with their newly-defined spatial neighbourhood and the most abnormal ones are classified as defective  
18 observations based on a density-based clustering algorithm. The approach was conceived to be as non-parametric  
19 and automated as far as possible to pre-process a growing number of datasets without supervision. The proposed  
20 approach showed promising results on real yield datasets with the detection of well-known sources of errors such  
21 as filling and emptying times, speed changes and non-fully used cutting bar.

22

23 **Keywords:** DBSCAN algorithm, filtering, local outliers, on-board sensors, spatial neighbourhood, yield

24

## 25 Introduction

26 Yield maps have been extensively recognized as a valuable source of information for field decision making (Diker  
27 et al. 2004; Florin et al. 2009; Pringle et al. 2003). They effectively provide a global overview of the field spatial  
28 variability which makes it interesting to target areas or zones for variable rate management. As a combine harvester  
29 passes through a field, yield monitors acquire almost in real-time multiple yield measurements all over the field.  
30 At the same time, those data are associated with the GNSS positioning of the machinery which enables precise  
31 location of each one of these observations at the within-field level. As such, thousands of yield spatial observations  
32 are generated and are ready to be used in the decision-making process. While this considerable volume of data is  
33 critical for field management and decision-making, these datasets must be used with great caution. They effectively  
34 contain lots of defective observations or technical errors that need to be removed to ensure data quality (Arslan  
35 and Colvin, 2002; Blackmore and Moore, 1999). As a consequence, yield datasets are often severely filtered to  
36 make sure further analyses are not flawed (Robinson and Metternicht, 2005; Sudduth and Dummond, 2007; Sun  
37 et al. 2013). Several authors have described to what extent a yield map could evolve after removing abnormal  
38 values (Simbahan et al. 2004; Sudduth and Dummond, 2007). Griffin et al. (2008) have even shown that these  
39 latter observations were able to influence field management decisions.

40 These technical errors or defective observations have been largely documented in the literature. Lyle et al.  
41 (2013) have proposed a categorization of those latter errors into four major groups: (i) harvesting dynamics of the  
42 combine harvester, (ii) continuous measurements of yield and moisture, (iii) accuracy of the positioning system  
43 and, (iv) harvester operator. These technical errors are briefly described hereafter, in the previously defined order,  
44 along with methodologies that have been proposed by the scientific community to identify these defective  
45 observations.

- 46 • The harvesting dynamics of the machine include three different offsets, referred to as the lag time, filling time  
47 and emptying time (Blackmore and Moore, 1999). The lag time induces an offset between the actual and the  
48 true location in space of a yield observation because the yield is not measured simultaneously with the cutting  
49 of the crop. Some attempts have been made to determine this offset through (i) geostatistical methods (Chung  
50 et al., 2002), (ii) image processing techniques (Lee et al. 2012) and (iii) signal deconvolution (Arslan, 2008;

51 Reinke et al. 2011). The filling time at the start of a harvest pass leads to an under-estimation of the yield  
52 because the grain flow is increasing and still has not reached a plateau, i.e. the permanent regime. Therefore,  
53 yield measurements do not match the expected true yield values. At the end of a harvest pass, some grain  
54 might still continue to flow after the last crop was harvested and the lag time has been reached. As a  
55 consequence, the latest observations of a harvest pass are generally under-estimated. The methods that have  
56 been proposed so far are exclusively visual, i.e. the grain flow is plotted against the travel time or distance of  
57 the machine and the data located before or after the plateau are removed (Lyle et al. 2013; Simbahan et al.  
58 2004).

- 59  
60 • Continuous measurements relate to yield and moisture observations. So far, studies have focused on  
61 thresholds, mostly determined empirically, to identify measurement errors (Sudduth and Drummond, 2007;  
62 Taylor et al. 2007). Arslan and Colvin (2002) have reported sensor accuracies varying between 1 and 4%  
63 while other authors have found differences up to 10% depending on environmental conditions during data  
64 acquisition, e.g. steep slopes (Reitz and Kutzback, 1996). To overcome that issue, a couple of studies have  
65 focused on the impact of the combine harvester vibrations on the yield measurement accuracy (Hu et al. 2012;  
66 Jingtao and Shuhui, 2010).
- 67  
68 • The accuracy of the positioning systems can lead to (i) observations outside field boundaries, (ii)  
69 measurements at the same spatial location, i.e. co-located points, or (iii) deviations in space according to a  
70 predefined harvest pass (Blackmore and Moore, 1999). The two first types of errors are easily handled by  
71 removing the points outside the boundaries of the field or points with similar co-ordinates (Robinson and  
72 Metternicht, 2005; Simbahan et al. 2004). Some algorithms have been implemented to reconstruct precisely  
73 the harvest passes by studying the angles formed by consecutive points (Lyle et al., 2013). Suspicious points  
74 – those the combine harvester is not likely to have gone through – are removed from the dataset.  
75
- 76 • Last type of errors has to do with the harvester operator. First, large variations in speed are likely to have a  
77 major impact on the yield dataset quality (Arslan and Colvin, 2002; Sudduth and Drummond, 2007). Speed  
78 issues are generally processed the same way as yield and moisture, i.e. by setting thresholds to the whole  
79 dataset or only to neighbouring data (Lyle et al. 2013). The harvester operator is also likely to overlap  
80 consecutive or adjacent harvest passes which may result in yield measurement errors. Some authors have  
81 focused on this ‘not fully used cutting bar’ effect and have come up with vector-based pre-processing methods  
82 to take into account these overlaps, mainly by reconstructing harvesting polygons (Drummond et al., 1999).  
83 These vector-based methods are heavily dependent on the positioning accuracy of the GNSS device and  
84 require a large processing time. Other authors have proposed specific on-board systems, such as those based  
85 on ultrasonic sensors (Zhao et al. 2010). Finally, harvest turns and headlands are also responsible for bad yield  
86 estimates (Lyle et al. 2013). Studies dedicated to these last sources of errors – though limited in the literature  
87 – have focused on finding the points inside harvest turns or headlands by using distance or angle measures  
88 between consecutive points. Suspicious points are removed.

89 On-board sensors such as yield monitors generate an extremely large amount of observations. This considerable  
90 volume of observations requires the filtering approaches to be at the same time automated, very general and non-  
91 parametric (Simbahan et al. 2004; Spekken et al. 2013). The automation condition is fundamental with regard to  
92 the increasing size and number of yield datasets to process. For instance, it would not be conceivable for an  
93 operator or advisor to spend time on the correction of hundreds of possible within-field yield maps. General and  
94 non-parametric detection methods are also to be preferred because of the diversity of datasets that have to be  
95 processed. These datasets are effectively acquired through a variety of acquisition systems – machines, sensors –  
96 and on multiple crops, with different operators and under varying conditions of acquisition, e.g. topography or  
97 climate. It is therefore important to make sure that the approaches are able to deliver conclusive results whatever  
98 the dataset to be analysed. Even though new operating systems exist to improve the quality of yield datasets, e.g.  
99 ultrasonic sensors (Zhao et al. 2010), it can be argued that all the actual combine harvesters are far from being  
100 equipped with it. General methods are therefore also required to process datasets arising from multiple types of  
101 machines, whatever the level of additional equipment installed. It must be kept in mind that agronomic datasets  
102 are often included in complex processes of field management and decision-making, and are sometimes used as  
103 inputs in agronomic models. Data filtering methods have therefore to be robust enough so that the decision-making  
104 process is accurate and not flawed. A limitation of the actual literature is that most of the existing approaches are  
105 semi-automatic and rely on expert thresholds and filters. These last aspects might be problematical for the

106 processing of yield maps at a larger scale as filtering settings can be influenced by each map producer and as  
107 skilled operators might be required for a considerable amount of time (Spekken et al. 2013).

108 The principal contribution of this work is to propose a new holistic data-driven method to filter out defective  
109 observations from on-the-go yield datasets. To the best of the author's knowledge, very few general or holistic  
110 data filtering approaches have been dedicated to within-field yield datasets. The methodology is firstly formalised  
111 and described to set all the concepts and definitions related to the removal of defective observations in yield  
112 datasets. Then, an implementation of the methodology is proposed with an emphasis on the approach to be as  
113 automated and non-parametric as possible. Finally, the approach is tested on real datasets obtained from grain flow  
114 sensors mounted on combine harvesters.

115

## 116 On-the-go vehicle based datasets and spatial outlier detection

### 117 Acquiring observations with on-board sensors

118 In agriculture, data acquisition with on-board sensors can be understood as a sequential procedure through time  
119 during which a machine acquires information of a variable  $Z$  in space. Indeed, the data collection process follows  
120 a temporal dynamic, i.e. observations are recorded in a specific order and one at a time as the machine passes  
121 through the field (Fig. 1). The machine can simply be modelled by a structuring element that moves through the  
122 field, e.g. a rectangle whose dimensions are defined by the characteristics of the machine and the associated on-  
123 board sensors. On-the-go measurements are punctual observations, i.e. diverse realisations of  $Z$ , and each point  
124 synthesizes the response of  $Z$  over the corresponding structuring element. The spatial resolution of the sensed  
125 variable is controlled by the distance between consecutive records and determined by the distance between adjacent  
126 passes of the machine. The spatial distance between consecutive observations is related to the speed of the machine  
127 and the sampling frequency. In a given field, this frequency of acquisition is generally stable which means that the  
128 distance between consecutive records only relies on the travel speed of the machine. On the other hand, the distance  
129 between adjacent passes depends on multiple parameters such as the work of the machine, the crop being sensed,  
130 or the cost of data acquisition among others. For instance, when a combine harvester with an on-board grain yield  
131 monitor passes through a field, the distance between adjacent passes is related to the width of the cutting bar  
132 because the whole field has to be harvested.

133

134

135

136

137

138

139

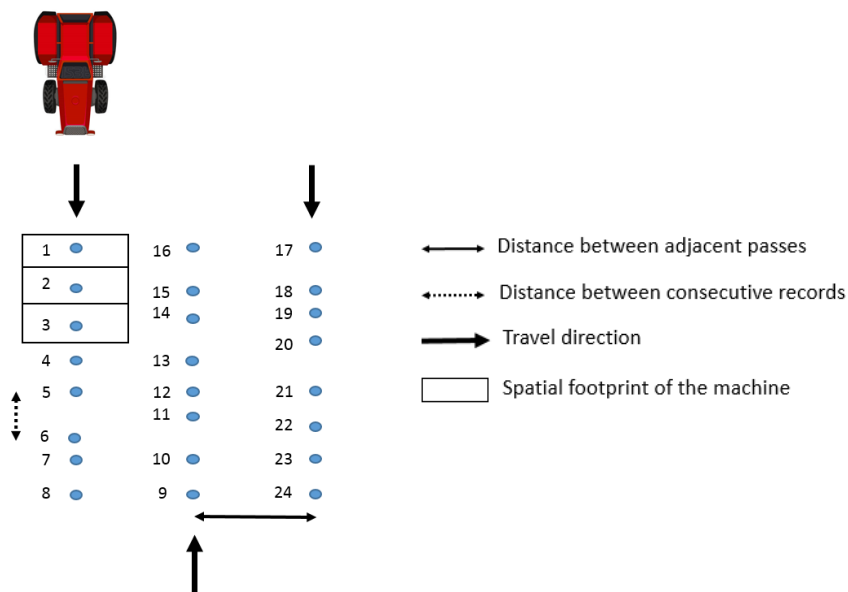
140

141

142

143

144



145 **Fig. 1.** Principle of data acquisition with on-board sensors.

146 According to Tobler's first law of geography, everything is related to everything else, but near things are  
147 more related than distant things (Tobler, 1970). This concept assumes that there exists some spatial correlation  
148 between spatially close observations, to a greater or lesser extent. Multiple studies have shown that this spatial

149 dependency has been clearly exhibited by yield datasets (Pringle et al. 2003; Simbahan et al. 2004). The presence  
150 of this spatial correlation is a central feature of the proposed filtering methodology.

151

## 152 Spatial outlier detection

153 The proposed approach will aim at removing the observations that are the cause of strong local variations of  $Z(x)$   
154 which might mask the true spatial correlation between neighbouring points. This approach can therefore be seen  
155 as a spatial outlier detection problem. Outlier detection is one of the major areas of investigation of the data mining  
156 community and has extended to numerous applications such as fraud detection, traffic networks or military  
157 monitoring (Ben-Gal, 2005; Gogoi et al. 2011). Hawkins (1980) has proposed a formal definition of an outlier  
158 which states that it can be described as an observation that deviates so much from the rest of the observations as  
159 to arouse suspicions that it was generated by a different mechanism. When observations are located in space, their  
160 spatial attributes, i.e. co-ordinates, can be used to define a spatial neighbourhood, known as a group of observations  
161 that are relatively close in space. A spatial outlier can then be defined as an observation whose non-spatial attributes  
162 behave differently to those of other observations in its spatial neighbourhood. From these two definitions arises  
163 the distinction between global and local outliers (Chen et al., 2008). Indeed, spatial outliers are only investigated  
164 in a spatial neighbourhood, meaning that the non-spatial attributes of outliers do not necessarily deviate from the  
165 entire dataset. On the contrary, the definition of an outlier proposed by Hawkins (1980) assumes a specific  
166 behaviour of an observation with regard to the whole dataset.

167 Spatial outlier detection has gained much interest with the increasing amount of spatial observations available.  
168 Although many more algorithms have been proposed to deal with traditional outliers, i.e. observations with no  
169 reference in space, several methods have been specifically addressed to the detection of spatial outliers (Chen et  
170 al. 2008; Filzmoser et al. 2014; Harris et al. 2014; Lu et al. 2003). These approaches generally involve three major  
171 steps. First, for each observation  $x_i$ , a spatial neighbourhood  $N(x_i)$  needs to be associated with each observation.  
172 To do so, the user can either define a spatial distance beyond which observations are no longer part of the spatial  
173 neighbourhood or select the number of  $k$  spatially close observations that belong to the spatial neighbourhood of  
174 each observation ( $k$  nearest neighbours). The next step in spatial outlier detection is the computation of a metric  
175 to quantify the difference between the non-spatial attributes of each observation and those of its spatial  
176 neighbourhood. This problem has been well formalized by Lu et al. (2003). Let  $f_A$  be an attribute function such  
177 that  $f_A(x_i)$  is the value of the attribute  $A$  of  $x_i$ . Let  $g_A$  be an attribute function such that  $g_A(x_i)$  is a summary statistic  
178 of the attribute  $A$  of the observations belonging to  $N(x_i)$ . A comparison function  $h_A$  can then be defined as a function  
179 of  $f_A$  and  $g_A$  to measure the ‘outlierness’ of each observation  $x_i$  with regard to  $N(x_i)$ . The ‘outlierness’ reports to  
180 what extent a given observation can be considered an outlier. A high indicator of ‘outlierness’ means that an  
181 observation is likely to be of low quality and as such can be regarded as a defective observation. As an example,  
182 Lu et al. (2003) have proposed a function  $g_A$  that returns the median of the attribute  $A$  of all the observations inside  
183  $N(x_i)$  and  $h_A$  was defined as  $f_A - g_A$ . Finally, the observations are directly classified as outliers or normal  
184 observations (Chen et al., 2008), or at least they are ordered from the most to the least suspicious observation  
185 (Filzmoser et al. 2014; Lu et al. 2003). In the last case, a threshold has to be manually selected to separate the  
186 outliers from the non-outliers.

187 The definition of outliers in on-the-go vehicle-based datasets such as yield datasets has not been stated so  
188 far and there is a need to be more specific about it. Observations can be considered as outliers if they are  
189 significantly different from their neighbouring observations. From a general perspective, outliers are removed from  
190 the datasets because they can negatively impact the quality of the entire population of observations. These outliers  
191 are often the result of a sensor error or a very particular and isolated phenomenon, e.g. game damage. However,  
192 in the case of sensors embedded on mobile machines, some outliers arise from the machine pass in itself, i.e. from  
193 the data collection process. These types of observations are different from their neighbouring observations, not  
194 because they are abnormal but rather because these observations were acquired under a specific acquisition  
195 process. For instance, when the cutting bar of a combine harvester is not fully used during a machine pass, yield  
196 observations are under-estimated because the grain flow is weighed over a harvest area that is bigger than it should  
197 be (Arslan and Colvin, 2002; Lyle et al. 2013).

198

199

200

201

202

### 203 Material and methods

204 A new data filtering algorithm dedicated to on-board sensor measurements

205 *A specific neighbourhood for each observation*

206 Spatial neighbours are observations that are relatively close to each other in the space domain. When acquiring  
 207 observations with on-board sensors, the data collection process follows the passes of the machine. This means that  
 208 spatially close observations might have been acquired (i) during a short time interval, i.e. these observations belong  
 209 at least to the same machine pass, or (ii) at different time periods, i.e. they belong to different passes. Given the  
 210 varying machine dynamics through the passes, spatially close observations in the same pass do not necessarily  
 211 have the same characteristics as spatially close observations in adjacent passes. In fact, it is reasonable to assume  
 212 that the data collection process induces in itself an anisotropic phenomenon in the direction of the machine pass,  
 213 i.e. between observations that belong to the same pass. This phenomenon should be taken into account separately  
 214 in the definition of the neighbourhood for each observation. As a consequence, the proposed approach attempts to  
 215 remove the observations that are the cause of strong local variations of  $Z$  which might mask the true correlations  
 216 between spatially close observations (i) in the same pass of the machine and (ii) in different passes of the machine.

217 More formally, the spatial neighbourhood  $N(x_i)$  of an observation  $x_i$  can be separated into two different  
 218 neighbourhoods: a spatio-temporal and a spatio-not-temporal neighbourhood. The spatio-temporal neighbours of  
 219  $x_i$  are the spatial neighbours that are, at the same time, near in space and time to  $x_i$ . An observation  $x_i$  and its spatio-  
 220 temporal neighbours are acquired in a short time interval. Spatio-not-temporal neighbours are near observations  
 221 in the space domain but not in the time domain. From now on, spatio-temporal and spatio-not-temporal neighbours  
 222 will be referred to as ST and SNT neighbours. Hence, for each observation  $x_i$ , the spatial neighbourhood  $N(x_i)$   
 223 is divided into  $ST(x_i)$  and  $SNT(x_i)$ . An example is given in Figure 2. Three passes are travelled in opposite directions.  
 224 Observation 13 has ST neighbours (observations 10, 11, 12, 14 and 15 for example) and SNT neighbours  
 225 (observations 2 to 7 and 18 to 23, for instance). The number of ST and SNT neighbours depends on the size of the  
 226 neighbourhood. Note that the use of the two neighbourhoods makes possible a distinction between the specific  
 227 machine dynamics inside the same pass and those in different passes of the machine.

228

229

230

231

232

233

234

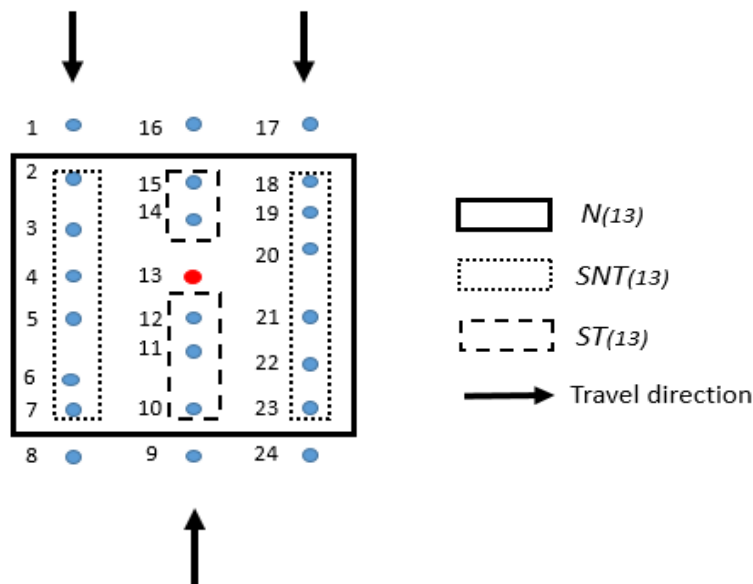
235

236

237

238

239



240 **Fig. 2.** ST and SNT neighbourhoods of an observation. Each observation  $x_i$  has a  $ST(x_i)$  neighbourhood  
 241 (observations are acquired in a short time interval) and a  $SNT(x_i)$  neighbourhood (observations belong to different  
 242 passes).

243 Given the spatial footprint of the machine and the sampling frequency, the spatial distance between  $x_i$  and the  
 244 observations inside  $SNT(x_i)$  is often larger than that between  $x_i$  and the observations inside  $ST(x_i)$ . If the spatial  
 245 neighbourhood of  $x_i$  is defined according to the  $k$  nearest neighbours, it may be difficult to control the amount of  
 246  $ST$  and  $SNT$  neighbours. As a consequence, it was decided to select the observations inside  $N(x_i)$  via a maximal  
 247 spatial distance below which observations belong to  $N(x_i)$ , and not to rely on a number of neighbours. This spatial  
 248 distance was set as a function of the distance between adjacent passes, e.g. the cutting width of the combine  
 249 harvester. Once observations inside  $N(x_i)$  were found, they were split between  $ST(x_i)$  and  $SNT(x_i)$ . To avoid  
 250 choosing a specific spatial distance for this neighbourhood research, observations inside  $N(x_i)$  were selected in  
 251 three different squared neighbourhoods of size two, three and four cutting widths of the machine. The algorithm  
 252 was then applied on each of these neighbourhoods and the results were averaged over them. It must be stated that  
 253 the use of these three spatial neighbourhoods gave three times more importance to the neighbours located at a  
 254 distance less than two cutting widths of the machines than to those located at a distance of four cutting widths of  
 255 the machine.

#### 256 *A robust metric to quantify the ‘outlierness’ of each observation*

257 Now that neighbouring relationships have been defined between observations, the spatial outlier-based  
 258 methodology can be put into place. Each observation  $x_i$  will be compared to the observations belonging to its two  
 259 different neighbourhoods, i.e.  $ST$  and  $SNT$  neighbours, to evaluate the ‘outlierness’ of  $x_i$ . As previously explained,  
 260 a large ‘outlierness’ value between an observation  $x_i$  and its  $ST$ ,  $SNT$  or both  $ST$  and  $SNT$  neighbours, indicates  
 261 that the attribute of  $x_i$  is significantly different to the attribute of its neighbours and therefore that  $x_i$  might be  
 262 considered as an outlier. As two neighbourhoods are considered for each observation, the attribute functions  $f_A$ ,  $g_A$   
 263 and the comparison function  $h_A$  can be computed twice. This leads to two measures of ‘outlierness’, one between  
 264  $x_i$  and the observations inside  $ST(x_i)$ , and the other between  $x_i$  and the observations inside  $SNT(x_i)$ . Given the  
 265 number of defective observations likely to be present in yield datasets, each observation  $x_i$  needs to be compared  
 266 to the observations inside  $ST(x_i)$  and  $SNT(x_i)$  with robust metrics not sensitive to outliers. To lessen the influence  
 267 of possible outliers inside  $ST(x_i)$  and  $SNT(x_i)$ , the attribute function  $g_A$  was set to return the median of the  
 268 observations belonging to  $ST(x_i)$  and  $SNT(x_i)$ . This summary statistic was proven to be effective in several studies  
 269 (Chen et al., 2008, Lu et al., 2003). The ‘outlierness’ measures are defined in the same way for  $ST(x_i)$  and  $SNT(x_i)$   
 270 with regard to  $x_i$ . The comparison function  $h_A$ , i.e. the ‘outlierness’ measure, was defined as follows:

$$271 \quad h_A = f_A - g_A \quad (1)$$

272 Where  $f_A$  and  $g_A$  are the attribute functions of the variable  $A$  corresponding respectively to observation  $x_i$  and the  
 273 observations inside  $ST(x_i)$  and  $SNT(x_i)$ ,  $h_A$  is the comparison function between  $f_A$  and  $g_A$ .

274

#### 275 *Bivariate plot of ‘outlierness’*

276 Each observation  $x_i$  is now characterized by two measures of ‘outlierness’ which can be represented in a bivariate  
 277 plot of ‘outlierness’ (Fig. 3). The bivariate plot does no longer contain spatial information, i.e. co-ordinates, which  
 278 means that the spatial outlier detection has now turned into a traditional outlier detection with a two-dimensional  
 279 dataset. Hence, from now on, all the notions of distances will only refer to distances between observations in the  
 280 bivariate plot, in the non-spatial attributes domain. From a general perspective, outliers can be defined as those  
 281 observations that have a strong disagreement with either  $ST$ ,  $SNT$  or both  $ST$  and  $SNT$  neighbours. Despite the  
 282 relatively high number of defective observations that can be found in datasets obtained from on-board sensors, the  
 283 majority of observations can be considered as non-outliers. These non-outliers, or normal observations, must have  
 284 similar characteristics to that of their  $ST$  and  $SNT$  neighbours and should all be found in the central portion of the  
 285 bivariate plot (Fig. 3). Indeed, normal observations have been given a small ‘outlierness’ measure in absolute to  
 286 indicate that their attribute value is really similar to that of their neighbours. Observations with large ‘outlierness’  
 287 values with regard to either  $ST$ ,  $SNT$  or both  $ST$  and  $SNT$  neighbours should be relatively far from the rest of the  
 288 observations and should be classified as outliers. All these observations must be now classified as outliers or non-  
 289 outliers to be able to automatically filter a high quantity of maps.

290

291

292

293  
294  
295  
296  
297  
298  
299  
300  
301  
302  
303  
304  
305  
306  
307  
308  
309  
310  
311  
312  
313  
314  
315  
316  
317  
318  
319  
320  
321  
322  
323  
324  
325  
326  
327  
328  
329  
330  
331  
332  
333  
334  
335  
336

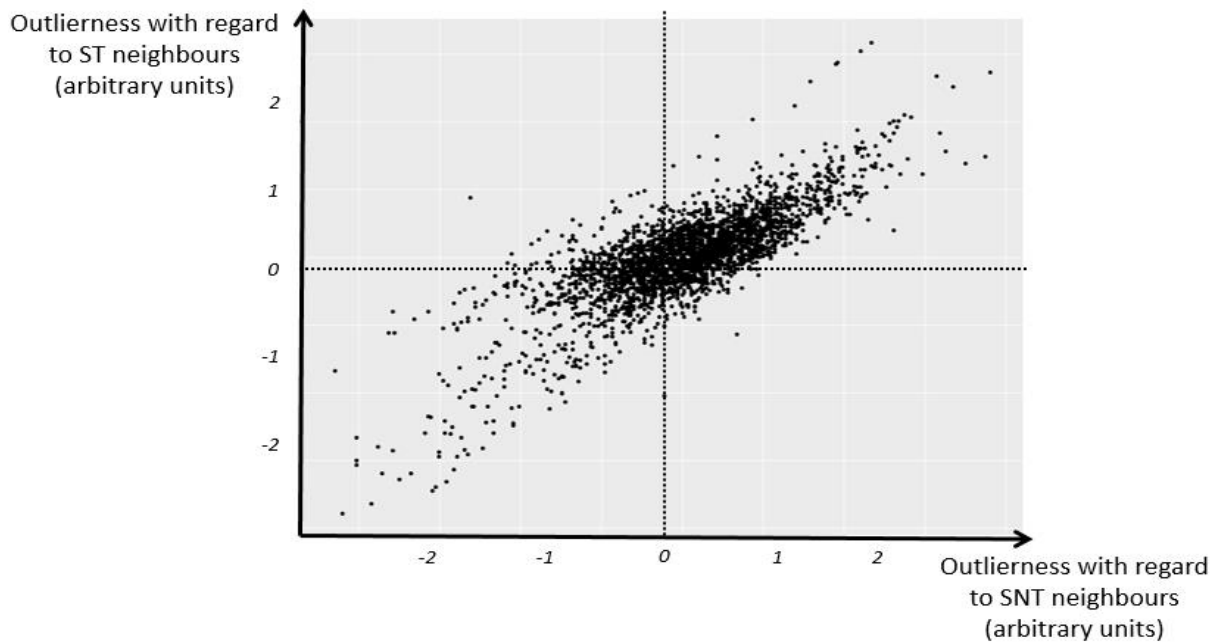


**Fig. 3.** ‘Outlierness’ of each observation with its ST and SNT neighbours. *The majority of observations in the centre of the plot have a small ‘outlierness’ value (relative to zero) with regard to their ST and SNT neighbours which indicates that these observations have a consistent behaviour with their neighbours.*

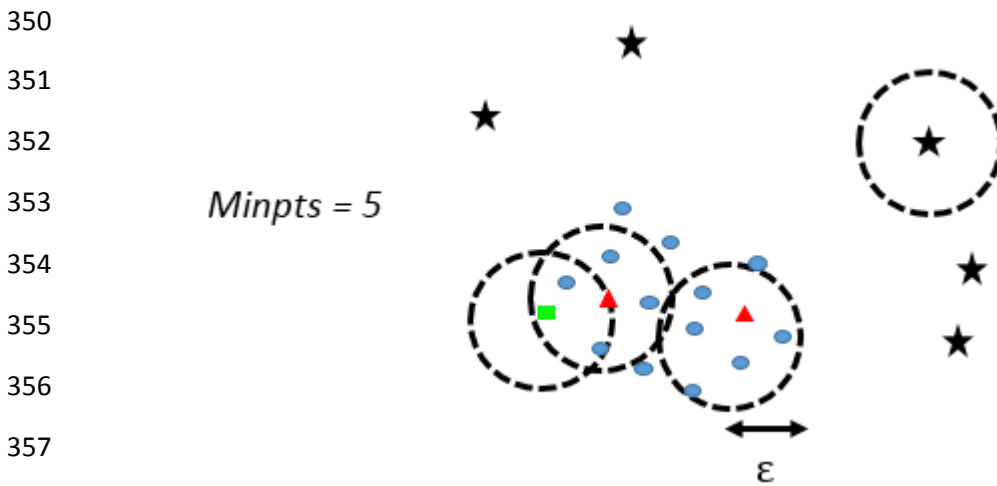
### *A density-based clustering algorithm*

As the majority of observations are considered non-outliers, the density of observations around normal observations should be much higher than around outliers (Fig. 3). Multiple density-based methods have been proposed in the literature but the threshold to classify observations as outliers or non-outliers is very often selected manually. As a consequence, it was decided to go further and to cluster observations that shared the same density of observations around them. One strong advantage of the clustering-based methods is that they do not give an ‘outlierness’ score to each observation but rather intend to discover groups of similar observations. On top of that, to automate the outlier identification, a non-parametric, or unsupervised, method should be preferred. Indeed, datasets acquired with on-board sensors are obtained through a variety of conditions, e.g. sensor, crop, operator, field characteristics, conditions of acquisition, and it was considered irrelevant to infer or consider a specific data distribution. A non-parametric method was also needed to deal with any arbitrary shape of the data distribution that was likely to occur. The algorithm DBSCAN (Density-Based Spatial Clustering of Applications with Noise) was selected because of its ability to combine both advantages of density and clustering-based approaches (Ester et al., 1996). This method also fulfils the constraints that were set previously, especially regarding the use of a non-parametric approach to classify the observations. Duan et al. (2007) proposed some improvements of the DBSCAN algorithm but they were not considered very useful in this outlier detection case. Other traditional methods commonly reported, i.e. distribution-based or distance-based (Filzmoser et al. 2014; Harris et al. 2014), might have been used but they were considered difficult to automate and to use in a non-parametric manner. Indeed, distribution-based methods rely on strong statistical assumptions with regard to the distribution of the variable of interest. Distance-based methods often require the variable distribution to be normal so that reliable thresholds can be used to classify observations as outliers (Filzmoser et al., 2014).

DBSCAN requires two parameters to identify clusters: the distance from each observation to its neighbours ( $\epsilon$ ) and the minimum number of observations inside the neighbourhood given the distance  $\epsilon$  (*Minpts*) (Fig. 4). It must be clear that the DBSCAN algorithm is applied on the bivariate plot of ‘outlierness’ and not on the initial dataset. To avoid any confusion with the neighbourhood  $N(x_i)$  previously introduced, this new neighbourhood of an observation  $x_i$  will be referred to as  $NO(x_i)$ , i.e. Neighbourhood with regard to ‘Outlierness’ values. For a given observation  $x_i$ , the algorithm finds its neighbouring observations  $NO(x_i)$  given the distance  $\epsilon$  and tests whether this  $NO$  neighbourhood contains at least *Minpts* observations (Fig. 4). When this condition is



337 fulfilled,  $x_i$  is set inside the core of a cluster and the algorithm expands the cluster by applying the same method to  
 338 the observations inside  $NO(x_i)$  and their corresponding neighbours until the constraint relative to  $Minpts$  is no  
 339 longer respected. For instance, in Figure 4, the triangles have at least five neighbours within an  $\varepsilon$  distance and  
 340 therefore are included in the core of the cluster. The square is reachable by one of the triangles, but this square has  
 341 less than five neighbours. The stars are not reachable by any point inside the core of the cluster and will not be  
 342 part of the central cluster. If an observation  $x_j$  is inside the neighbourhood of an observation  $x_i$  but the  
 343 neighbourhood of  $x_j$  contains less than  $Minpts$  observations, observation  $x_j$  is labelled as noise but is still included  
 344 in the cluster corresponding to  $x_i$ , e.g. the square in Fig. 4 (Ester et al., 1996). The insertion of  $x_j$  in the cluster  
 345 related to  $x_i$  helps retrieve the global shape of the cluster rather than the core of the cluster only. This method was  
 346 considered appropriate to build one large cluster retaining all the normal observations while leaving the outliers in  
 347 other clusters. To obtain a reliable clustering, it was necessary to define the optimal parameters  $\varepsilon$  and  $Minpts$ .  
 348 Some works had already been proposed to determine automatically these criteria but still requires some manual  
 349 thresholds (Sawant, 2014). The previous work helped to develop a fully-automated approach.



359 **Fig. 4.** Application of the DBSCAN algorithm.

360 The distance  $\varepsilon$  was defined in the first place as the most frequent distance between two different  
 361 observations (Fig. 7). In fact, as the majority of observations, i.e. the non-outliers, are expected to be clustered in  
 362 the same group, the most frequent distance between two different observations should be a characteristic of normal  
 363 observations. The distances were calculated as euclidean distances between two observations within the bivariate  
 364 plot of ‘outlierness’ (Fig. 3). The ‘outlierness’ measures were centred and reduced to avoid giving too much  
 365 influence to one of these two measures of disagreement. Given this optimal  $\varepsilon$  distance, the number of neighbours  
 366 inside  $NO(x_i)$  was computed for each observation  $x_i$ . The distribution of the  $NO$  neighbours was used to select an  
 367 optimal value for the  $Minpts$  parameter (Fig. 7). As the  $Minpts$  value increases, the size of the clusters diminishes  
 368 because less and less observations fulfil the requirement regarding the minimum number of observations inside  
 369 their neighbourhood. This  $Minpts$  parameter must not be set too high so that the whole shape of the cluster is taken  
 370 into account. It was stated that a break in the  $NO$  neighbours’ distribution should reflect an optimal separation  
 371 between different clusters. This break was chosen to be a local minimum in the distribution of the  $NO$  neighbours.  
 372 Indeed, a local minimum corresponding to  $k$  neighbours indicates that the observations that have  $k$  neighbours  
 373 within a  $\varepsilon$  distance are located at the border between two clusters of different density of neighbours. This first local  
 374 minimum was considered a good indicator of the separation between normal and outlying observations. To  
 375 optimally select the parameters  $\varepsilon$  and  $Minpts$ , the densities of (i) the distance between different observations and  
 376 (ii) the number of neighbours for an optimal  $\varepsilon$  distance, were estimated via a kernel density estimation (KDE).

377

#### 378 *Adjusted filtering for wrongly identified outliers*

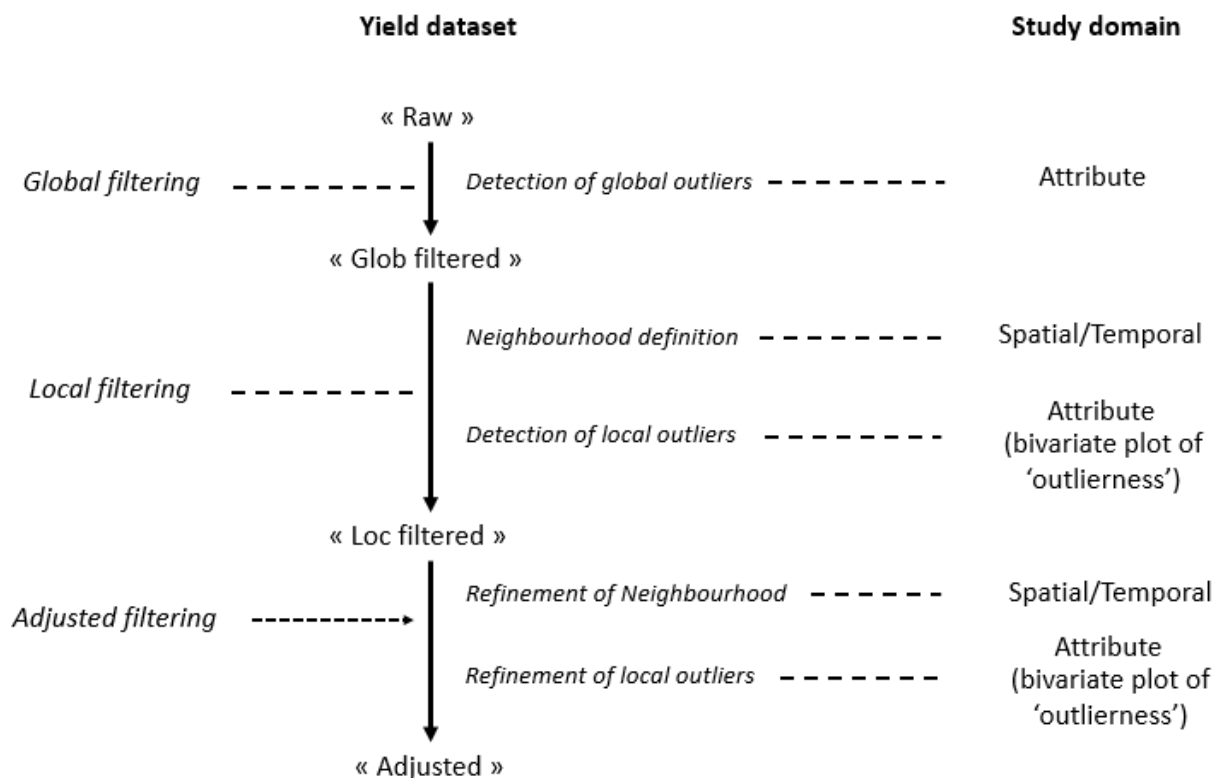
379 When the ST and SNT neighbourhoods of an observation  $x_i$  contain many defective observations, the function  $h_A$   
 380 might be sensitive to these outliers, even if robust metrics are used. As a consequence, some observations might  
 381 be wrongly classified as outliers only because their neighbourhood is outnumbered by outliers. To overcome this

382 limitation, the ‘outlierness’ values attributed to each observation  $x_i$  that was previously classified as an outlier has  
 383 to be re-evaluated. More specifically, each observation must be compared to a neighbourhood that only contains  
 384 non-outlying observations considering the first iteration of the approach. In this way, the influence of outliers in a  
 385 spatial neighbourhood is removed. To account for the wrongly identified outliers, a second iteration of the  
 386 proposed approach was put into place. For each observation  $x_i$ ,  $h_A(x_i)$  was recalculated except that this time, the  
 387 neighbourhoods of  $x_i$  were set free of other outliers. This means that if an observation is definitely an outlier,  
 388 removing outliers from its neighbourhood will still classify this observation as an outlier. On the other hand, if the  
 389 observation was wrongly classified as an outlier, removing outliers from its neighbourhood would significantly  
 390 decrease the ‘outlierness’ values associated and therefore would lead to classifying the observations as a normal  
 391 one. Once each observation  $x_i$  was given new  $h_A(x_i)$  values with regard to both ST and SNT neighbours, the  
 392 classification based on the DBSCAN algorithm was run a second time to identify the real outliers.

393 *Last considerations before using the proposed algorithm*

394 The adjusted spatial outlier detection was not applied directly on the raw dataset. Some corrections were added  
 395 before applying the proposed algorithm to improve the quality of the results. Among the observations that were  
 396 likely to affect the efficiency of the proposed algorithm, especially co-located points and global outliers were of  
 397 great concern and were removed before searching for spatial outliers. Co-located records are observations that are  
 398 acquired at the same spatial position either due to a stop of the combine or to an error in the GNSS position. In  
 399 either case, these observations must be filtered out because they exhibit most likely an abnormal value. Global  
 400 outliers were removed because they could be spotted relatively easily and could have some influence on the  
 401 detection of the spatial outliers. Global outliers were removed in a non-parametric way following the method of  
 402 Hubert and Van der Veecken (2008).

403 To ease the understanding of the proposed approach and knowing that the procedure requires to travel between  
 404 multiple domains, i.e. spatial, temporal, and attribute, a flowchart of the algorithm is provided (Fig. 5). A step-by-  
 405 step description of the data filtering process is also presented afterwards.



406

407

408 **Fig. 5.** A simple flowchart of the proposed approach

409

#### 410 **Algorithm (Adjusted Spatial Outlier detection)**

- 411 1. Remove co-located points and global outliers [*Global filtering*]
- 412 2. Remove local outliers [*Local filtering*]
- 413 a. For each point  $x_i$  remaining in the dataset:
  - 414 i. Compute the square neighbourhoods based on a radius of two, three and four cutting
  - 415 widths. For each of these neighbourhoods:
    - 416 1. Separate the neighbourhood  $N(x_i)$  into  $ST(x_i)$  and  $SNT(x_i)$
    - 417 2. Calculate the ‘outlierness’ value of  $x_i$  with regard to  $ST(x_i)$  and  $SNT(x_i)$  using
    - 418 the function  $h_A$
  - 419 ii. Average the ‘outlierness’ values with regard to  $ST(x_i)$  and  $SNT(x_i)$  over the three square
  - 420 neighbourhoods
- 421 b. Determine optimal parameters  $\varepsilon$  and  $Minpts$  for the DBSCAN algorithm
- 422 c. Apply DBSCAN to extract the cluster consisting of normal observations
- 423 3. Refine detection of local outliers [*Adjusted filtering*]
- 424 4. Extract the final cluster of normal observations.
- 425

426 The whole methodology was developed using the R statistical environment (R Core Team, 2013).

427

#### 428 Evaluation of the proposed algorithm and datasets used

429 The proposed algorithm was tested on ten real within-field yield datasets arising from three different farms, i.e.  
430 two located near Evreux, in the north-western part of France (Farm 1 - WGS84: E:0.779, N:48.955; Farm 2 -  
431 WGS84: E:1.032, N:48.828) and one located close to Peterborough, UK (Farm 3 - WGS84: E:-0.105, N:52.643).  
432 Fields were mostly cropped in wheat and harvested with combines of different brands, especially New Holland  
433 (Turin, Italy) and Claas (Harsewinkel, Germany) combines. Among these ten datasets, two of them (dataset 1 from  
434 Farm 3 and dataset 2 from Farm 2) were selected to provide readers with a deeper analysis of the proposed  
435 approach. The two datasets (datasets 1 and 2) were especially chosen for containing different sources of defective  
436 observations. Table 1 and 2 respectively report yield statistics for the two (datasets 1 and 2) and ten datasets under  
437 consideration.

438 For the ten yield datasets, the proposed approach was evaluated in the same way as in many previous studies, i.e.  
439 by looking at the yield distribution and spatial structure before and after filtering out outliers (Simbahan et al.,  
440 2004, Sudduth et al., 2007). This evaluation procedure still has some limits as this validation remains somehow  
441 qualitative. Indeed, outliers are not labelled in the yield datasets so one cannot be entirely sure whether an outlier  
442 is truly one. However, this procedure was considered sufficient in the first instance. Furthermore, for datasets 1  
443 and 2, the detected outliers were plotted on their corresponding field to better understand their characteristics.

444

#### 445 **Results and discussion**

446 Improvements in the yield distribution and spatial structure

447 *A specific attention to datasets 1 and 2*

448 Both raw and filtered yield datasets of datasets 1 and 2 are presented via their principal descriptive statistics (Table  
449 1) and semi-variograms (Fig. 6). The pre-filtering step, i.e. *Glob outliers*, consisted in the removal of co-located  
450 points and global outliers. Observations with a yield value equal to zero were also discarded because they were  
451 likely to mask the presence of some global outliers. Indeed, observations with a zero yield value are definitely not  
452 expected and might have been obtained when the cutter bar was lowered while the crop had already been harvested.  
453 The removal of zero yield values, co-located points and global outliers substantially changed the summary statistics  
454 of yield datasets by lowering the standard deviation by a factor of 2 and increasing the average yield in the fields  
455 by almost 5%. More interestingly, these first outliers were completely masking the yield spatial structure in the  
456 two fields of interest (Fig. 6). Indeed, the semi-variograms testify of a clear yield spatial structure with well-defined  
457 nugget and sill parameters. These results demonstrate to what extent a simple pre-filtering approach such as the  
458 removal of global outliers and really unexpected values (zero-yield observations) can improve the characteristics  
459 of within-field yield datasets.

460

461 **Table 1.** Yield descriptive statistics ( $t\ ha^{-1}$ ) of datasets 1 and 2. ‘Raw’ stands for the original dataset. ‘Glob filtered’  
 462 is the original dataset after the pre-filtering step (essentially global outliers, co-located points and zero-yield  
 463 observations. ‘Loc filtered’ is the dataset after the pre-filtering step and the removal of local outliers. ‘Adjusted’  
 464 is the dataset after adjustment for wrongly identified outliers. SD stands for standard deviation. Nb. observations  
 465 is the number of observations in the corresponding dataset.

Dataset	Type	Min	Mean	Median	Max	SD	Nb. observations
1	Raw	0	7.75	8.13	90.41	2.65	6526
	Glob filtered	3.20	8.04	8.20	11.64	1.38	6143
	Loc filtered	4.26	8.26	8.32	11.31	1.04	5333
	Adjusted	4.56	8.26	8.31	11.37	1.06	5400
2	Raw	0	8.65	9.10	40.00	1.99	3279
	Glob filtered	5.80	9.07	9.20	11.20	0.87	3003
	Loc filtered	6.80	9.16	9.20	11.20	0.68	2743
	Adjusted	6.80	9.16	9.20	11.20	0.70	2803

466

467 Local outliers were removed from the previously pre-filtered dataset (*Loc filtered*). These outliers have  
 468 less influence on yield summary statistics compared to the global outliers (Tab. 1). This is essentially due to the  
 469 fact that these statistics characterize the yield dataset at a global level. However, it can be seen that local statistics  
 470 are substantially impacted by these local outliers (Fig. 6). The spatial structure appears effectively much more  
 471 clearly once outliers have been removed. As expected, the final step of the proposed methodology, i.e. *Adjusted*,  
 472 does not produce major improvements on either the yield distribution or spatial structure. This step can rather be  
 473 considered like a refinement of the proposed approach and was not aimed to drastically impact the yield  
 474 characteristics.

475

476

477

478

479

480

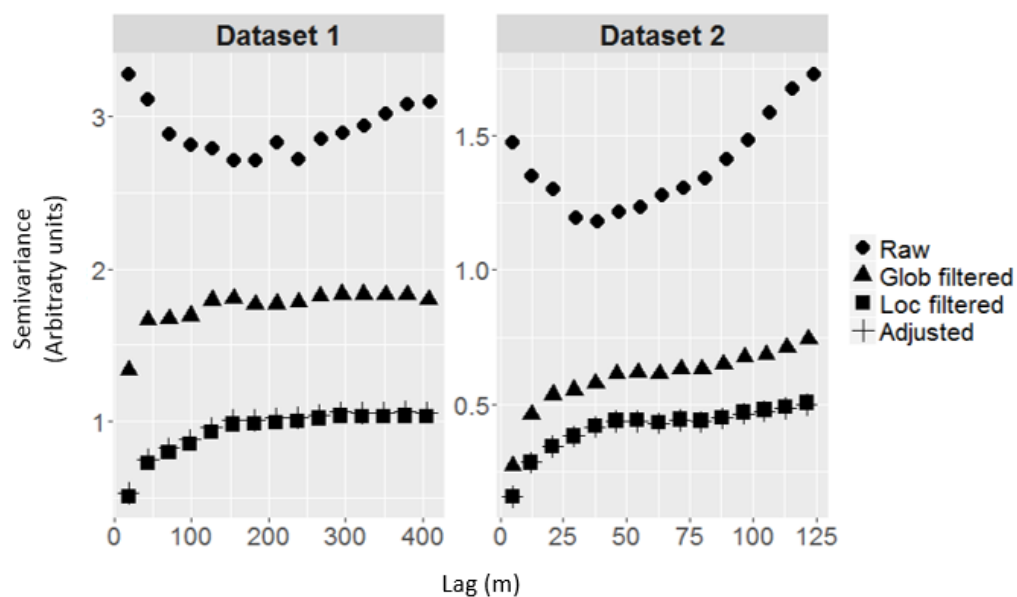
481

482

483

484

485



486 **Fig. 6.** Spatial structure of yield datasets 1 and 2 with the proposed methodology. ‘Raw’ stands for the original  
 487 dataset. ‘Glob filtered’ is the original dataset after the pre-filtering step (essentially global outliers, co-located  
 488 points and zero-yielding observations. ‘Loc filtered’ is the dataset after the pre-filtering step and the removal of  
 489 local outliers. ‘Adjusted’ is the dataset after adjustment for wrongly identified outliers.

490

491 *Analysis of the ten datasets under study*

492 Table 2 reports descriptive and spatial statistics regarding the ten datasets under consideration. All the raw yield  
 493 datasets exhibit a large variability, i.e. high coefficient of variation, because of the presence of global and local  
 494 defective observations. The influence of local outliers on the yield spatial structure is clear for all the ten datasets  
 495 under study (Table 2). Indeed, nugget to sill ratios are significantly improved, i.e. reduced, once local outliers are  
 496 filtered out from the yield datasets. Even though the level of autocorrelation remains medium for some datasets  
 497 after the removal of local outliers, e.g. nugget to sill ratio more than 50%, it must be clear that the spatial structure  
 498 is still stronger than when local outliers were left inside the yield datasets. The proposed methodology removed a  
 499 relatively high number of observations, i.e. from 19 to 50% of the dataset size (Table 2). These defective  
 500 observations are, at the same time, global and local outliers, and with different proportions of each type for each  
 501 dataset. Some datasets effectively contain more global outliers, e.g. because of more measurements when the  
 502 cutting bar was up, while more local outliers have been filtered in others, e.g. more speed changes. Note also that  
 503 this number of defective observations substantially varies among the datasets under study which demonstrates that  
 504 all yield datasets are different and that a general filtering methodology is interesting to consider.

505 **Table 2.** Yield statistics for the ten datasets under consideration. *Spatial statistics are presented before (Glob*  
 506 *filtered) and after (Loc Filtered) removing yield local outliers. The percentage of points removed during the whole*  
 507 *filtering process (from 'raw' to 'adjusted' yield datasets) is also reported. CV stands for the coefficient of*  
 508 *variation.*

Dataset	Descriptive statistics (Raw yield dataset)			Spatial statistics		
	Surface (ha)	Mean (t.ha <sup>-1</sup> )	CV (%)	Nugget/Sill (%) <i>Glob filtered</i>	Nugget/Sill (%) <i>Loc Filtered</i>	Points removed (%)
1	20.5	7.75	23.0	72	52	19
2	3.5	8.65	34.2	66	49	17
3	13.1	5.1	114	100	50	42
4	28.0	4.9	57.5	100	55	45
5	45.2	6.3	48.5	82	41	33
6	10.5	7.1	67.7	85	33	50
7	25.1	7.5	50.3	92	29	33
8	13.1	7.6	60.7	85	76	32
9	22.2	7.1	73.4	84	40	39
10	30.5	9.4	21.1	32	21	21

509

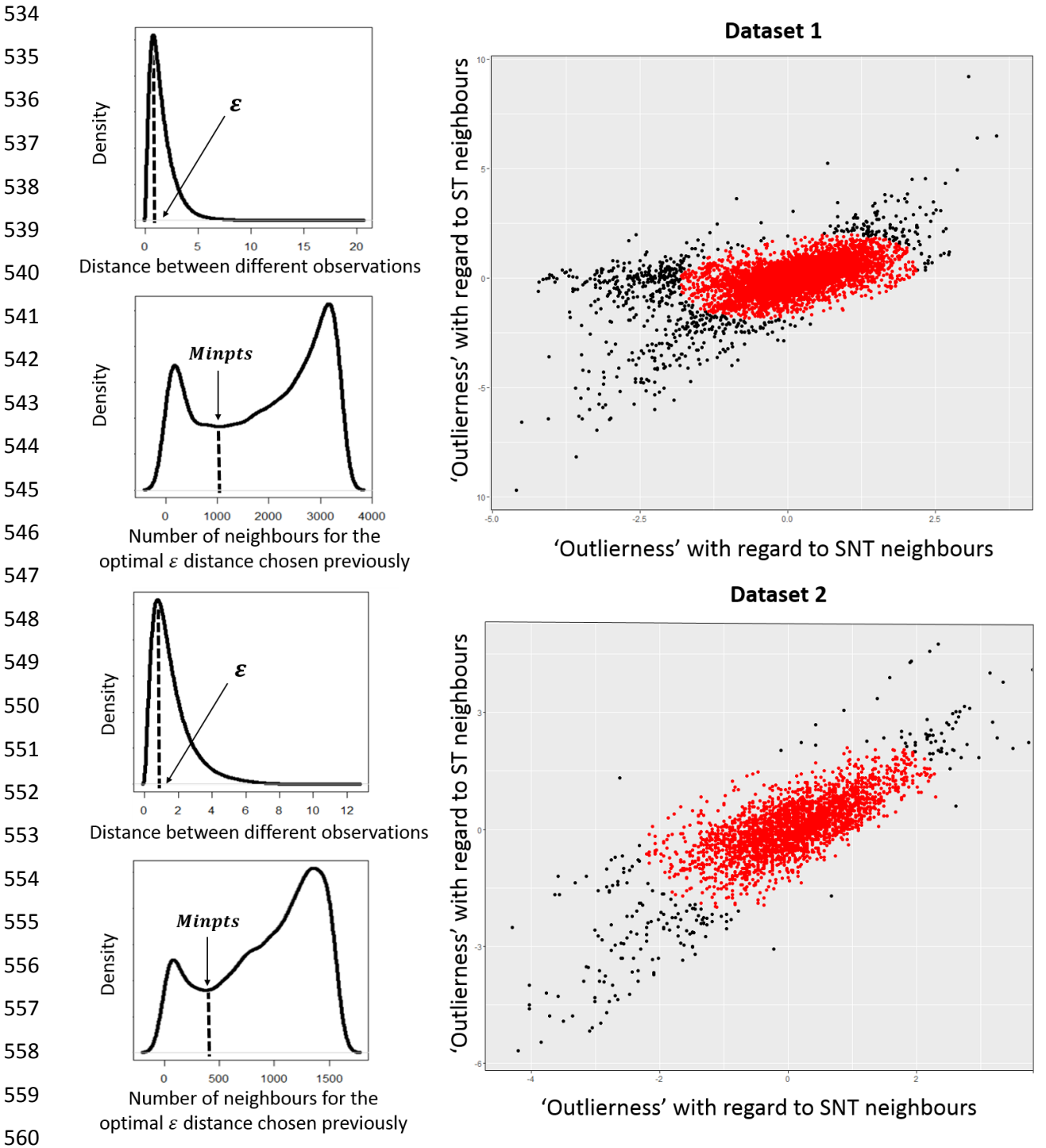
510 Evaluation of the density-based clustering approach

511 *Detection of the DBSCAN parameters*

512 Figure 6 demonstrates the application of the DBSCAN algorithm on the bivariate plot of 'outlierness' for datasets  
 513 1 and 2. For both datasets, there is a clear maximum value in the density of distances between different observations  
 514 which enables a clear detection of the  $\epsilon$  distance (Fig. 7, left). As the distance between different observations  
 515 increases, more and more distant observations are considered. Small distances between different observations  
 516 characterize essentially the nearest neighbour distances between observations inside the core of the cluster of  
 517 normal observations which is why the density is relatively low for these distances. The clear peak identifies the  
 518 distance between two different observations that is the most representative of the cluster of normal observations.  
 519 After the peak, the larger distances account for very distant observations such as, for instance, a normal observation  
 520 and an outlier, or two normal observations very far from each other inside the cluster of normal observations. The  
 521 most frequent distance between two different observations should therefore reliably discriminate the cluster of  
 522 normal observations.

523 For both datasets, the first local minimum in the density of the number of neighbours, i.e. corresponding  
 524 to the parameter *Minpts*, appears relatively clearly. For the optimal  $\epsilon$  distance that was previously chosen, as the  
 525 number of neighbours increases, the density of the number of neighbours starts decreasing relatively quickly then  
 526 increases smoothly at first, then more abruptly (Fig. 7, left). The first peak and neighbouring values is due to  
 527 outlying observations that have a few number of neighbours within an  $\epsilon$  distance. The last peak and neighbouring  
 528 values are related to normal observations, i.e. inside the core of the cluster of normal observations, with a very  
 529 high number of neighbours within an  $\epsilon$  distance. Between these two peaks, the first local minimum in the density  
 530 of the number of neighbours, from the lesser to greater number of neighbours, is considered a good separator

531 between the cluster of normal observations and the outliers. Indeed, it separates a high-density region from low-  
 532 density regions. The first local minimum is also generally the global minimum in the distribution of the *NO*  
 533 neighbours. It was therefore selected as a good estimate to separate outliers from normal observations.



561 **Fig. 7.** Optimal selection of DBSCAN parameters and corresponding detection of normal observations. *For each*  
 562 *dataset, the plot in the top left-hand corner helps determine the optimal  $\epsilon$  distance while that in the bottom left-*  
 563 *hand corner enables retrieval of the *Minpts* parameter of the DBSCAN algorithm. The right plot shows the cluster*  
 564 *of normal observations in the centre portion of the plot (red dots in the online version) and the outliers identified*  
 565 *by the proposed method.*

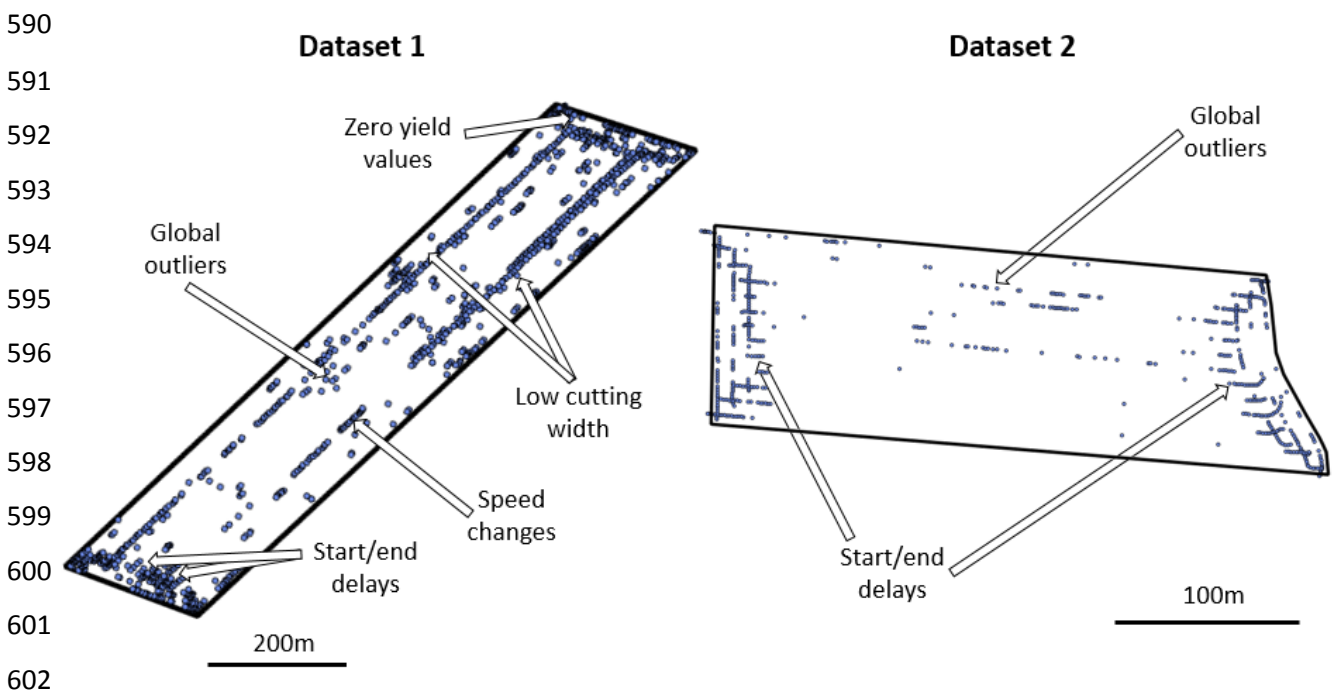
566 Be aware that the identification of the DBSCAN parameters, i.e.  $\epsilon$  and *Minpts*, was clear for the ten yield  
 567 datasets under consideration (data not shown) meaning that the outliers could be separated from the rest of the

568 observations. Depending on the type and number of defective observations, the shape of the density curves did not  
569 match perfectly but the overall structure was similar.

### 570 *Detection of local outliers*

571 Using the parameters previously defined, the DBSCAN algorithm was able to find a large and dense cluster in the  
572 centre of the data for both datasets (Fig. 7, right). Regarding dataset 1, some outliers expand towards the left of  
573 the plot and exhibit a large ‘outlierness’ value with regard to their SNT neighbours (value far from 0) and a low  
574 ‘outlierness’ value with regard to their ST neighbours. These outliers are observations that belong to passes  
575 harvested with a low cutting width (Fig. 8, left). Indeed, a long tail of low-yielding observations surrounded by  
576 observations with a much higher yield value is very often the sign of a non-fully used cutting bar. These  
577 observations are consistent with spatially close observations in the same pass because all of them were recorded  
578 with a low cutting width. In contrast, adjacent passes were harvested with a full cutting bar which is why these  
579 outliers do not share similar characteristics with spatially close observations in adjacent passes.

580 For the two fields under study, some outliers are located on the diagonal of the plot, i.e. the yield values  
581 of these observations are significantly different from those of their ST and SNT neighbours. This characteristic is  
582 specific to observations recorded at the start and end of each row (Fig. 8). When the combine harvester enters or  
583 leaves a pass, the grain flow can be significantly different from within the pass. The filling time at the start of a  
584 harvest pass induces an under-estimation of the yield because the grain flow is increasing and still has not reached  
585 a plateau, i.e. within the pass. Therefore, the yield measurement does not match the expected true yield. At the end  
586 of a harvest pass, some grain might still continue to flow after the last crop was harvested and the lag time has  
587 been reached. As a consequence, these observations have a different behaviour to that of spatially close  
588 observations in the same and in adjacent passes. These two known sources of error are the most easily detected on  
589 the right-hand side plot because the corresponding observations are relatively clustered on the plot.



603 **Fig. 8.** Location and label of the outliers detected by the proposed methodology within the fields.

604 In contrast to the two previous sources of errors, some outliers are detected more irregularly in the field  
605 and might be the sign of abrupt speed changes or bad moisture/yield records. Some of these other sources of error,  
606 e.g. speed changes can also be identified relatively precisely. From a practical point of view, the yield is the ratio  
607 of the grain flow to the corresponding harvested area during a fixed time interval. A harvest area can be defined  
608 by both the cutting width and the travel speed of the machine. As a consequence, large speed variations during a  
609 specific time interval result in large yield variations. Observations acquired during a speed change will likely have  
610 different properties than those of spatially close observations in the same and in adjacent passes.

611           Regarding the ten datasets under study, each bivariate plot of ‘outlierness’ had its proper characteristics  
612 depending on the types of outlier present (data not shown). Some features were recurrent, e.g. the outliers located  
613 on the diagonal of the plot, because all the yield datasets contained observations related to the filling and emptying  
614 time of the machine, to a greater or lesser extent. Others were less present such as the tail of outliers expanding  
615 towards the left of the plot because overlaps were very rare within the datasets. From a general perspective, it is  
616 clear that each yield dataset has its own properties. This implies that there is a need for filtering procedures to be  
617 as flexible and general as possible so that each dataset can be processed accordingly no matter the type or number  
618 of outliers.

619           The proposed methodology has only been applied to the yield attribute in yield datasets. It could be argued  
620 that none of the other attributes in yield datasets, such as the speed of the machine or the grain moisture, had been  
621 used to detect the possible outliers. It was actually considered that all these attributes were used in the calculation  
622 of the yield attribute and therefore that any strong deviations of one of these attributes should have led to a bad  
623 yield estimate that would have been spotted as outliers with regard to its ST or SNT neighbours.

624           In this study, several outliers that were detected by the proposed algorithm were put in relation to some  
625 technical errors that can be found within yield datasets (Fig. 8). Nonetheless, it remains relatively difficult to assess  
626 the effectiveness of a specific filtering methodology. In fact, as raw yield observations are not labelled within the  
627 datasets, one cannot be entirely sure whether an observation identified as an outlier is truly one. Obviously, some  
628 errors are clearly visible on the map but for others, it is much more difficult to be sure, even with a skilled operator.  
629 To cope with this issue, one possibility could be to generate simulated yield datasets in which the location of  
630 outliers is known so as to assess more objectively the interest and reliability of a filtering approach (Leroux et al.,  
631 2017). Another improvement of the proposed methodology would be to intend to correct the outliers detected  
632 instead of abruptly removing them. Indeed, even if the removal of outliers is not dramatic for the size of the yield  
633 datasets as they already contain lots of observations, it could be still interesting to see whether a proper correction  
634 is possible. As it was found that multiple sources of error had a specific behaviour in the bivariate plot of  
635 ‘outlierness’, it might be conceivable to identify and label these errors so as to propose a correction. For instance,  
636 observations belonging to passes harvested with a low cutting width could be extracted and corrected properly by  
637 estimating the proportion of the cutting width that was actually used when these observations were acquired.

638

## 639 **Conclusion**

640           A new holistic data-driven method was proposed to filter out local outliers from within-field yield datasets. This  
641 approach essentially consisted in finding observations whose attribute of interest had the most significant  
642 difference with regard to that of the observations inside their spatial neighbourhood. To meet the specificities of  
643 within-field yield datasets, a new concept of neighbourhood has been formalised. Outlying observations were then  
644 detected by a density-based clustering method. One of the major interests of the approach is that it does not require  
645 any manual settings prior to the filtering. All metrics and thresholds are driven by the data themselves. The  
646 approach was successfully tested on yield datasets but could be extended to many more spatial datasets from on-  
647 the-go sensors. Besides, it must be said that the methodology was applied solely on the yield attribute, i.e. on  
648 univariate datasets. The approach could also be extended to datasets of higher dimension. Overall, the proposed  
649 algorithm was proven effective at removing unwanted observations from on-the-go vehicle-based yield datasets  
650 and should be used as a first step before deeper processing. Despite significant improvements in the distribution  
651 and spatial structure of yield datasets, the evaluation of the algorithm was still subjective. Future work will involve  
652 the comparison of multiple approaches through the use of simulated datasets to offer much more objective  
653 conclusions.

654

## 655 **References**

- 656 Arslan, S., & Colvin, T. (2002). Grain yield mapping : yield sensing, yield reconstruction, and errors. *Precision*  
657 *Agriculture*, 3, 135-154
- 658 Arslan, S. (2008). A Grain Flow Model to Simulate Grain Yield Sensor Response. *Sensors*, 8, 952–962.
- 659 Ben-Gal, I. (2005). Outlier Detection. *The Data Mining and Knowledge Discovery Handbook: A Complete Guide*  
660 *for Practitioners and Researchers*. Boston: Kluwer Academic Publishers.
- 661 Blackmore, B. S., & Moore, M. (1999). Remedial correction of yield map data. *Precision Agriculture* 1, 53–66.



662 Chen, D., Lu, C-T., Kou, Y. & Chen, F. (2008). On Detecting Spatial Outliers. *Geoinformatica*, 12, 455-475

663 Chung, S. O., Sudduth, K. A., & Drummond, S. T. (2002). Determining Yield Monitoring System Delay Time

664 With Geostatistical and Data Segmentation Approaches. *Transactions of the ASAE*, 45, 915-926.

665 Diker, K., D.F. Heerman, & M.K. Brodahl. (2004). Frequency analysis of yield for delineating yield response

666 zones. *Precision Agriculture*, 5, 435-444.

667 Drummond, S. T., Fraisse, C. W., & Sudduth, K. A. (1999). Combine Harvest Area Determination by Vector

668 Processing of GPS Position Data. *Transactions of the ASAE*, 42, 1221-1227.

669 Duan, L., Xu, L., Guo, F., Lee, J., & Yan, B. (2007). A local-density based spatial clustering algorithm with noise.

670 *Information Systems*, 32, 978-986

671 Ester, M., Kriegel, H.-P., Sander, J., and Xu, X. (1996). A density-based algorithm for discovering clusters in large

672 spatial databases with noise. In E. Simoudis, J. Han, and U. Fayyad (Eds.), *Proceedings of Second*

673 *International Conference on Knowledge Discovery and Data Mining*, Palo Alto, CA, USA: AAAI Press, pp

674 226-231.

675 Filzmoser, P., Ruiz-Gazen, A. & Thomas-Agnan, C. (2014). Identification of local multivariate outliers. *Statistical*

676 *Papers*, 55, 29-47.

677 Florin, M.J., McBratney, A.B., Whelan, B.M. (2009). Quantification and comparison of wheat yield variation

678 across space and time. *European Journal of Agronomy*, 30, 212-219.

679 Gogoi, P, Bhattacharyya D, Borah B, & Kalita JK (2011). A survey of outlier detection methods in network

680 anomaly identification. *Computer Journal*, 54, 570-88.

681 Griffin, T., Dobbins, C., Vyn, T., Florax, R., & Lowenberg-DeBoer, J. (2008). Spatial analysis of yield monitor

682 data: case studies of on-farm trials and farm management decision making. *Precision Agriculture*, 9, 269-

683 283

684 Harris, P., Brunson, C., Charlton, M., Juggins, S., & Clarke, A. (2014). Multivariate Spatial Outlier Detection

685 Using Robust Geographically Weighted Methods. *Math Geosciences*, 1-31.

686 Hawkins, D. (1980). *Identification of Outliers*, London, UK: Chapman & Hall

687 Hu, J., Gong C., & Zhang Z. (2012) Dynamic Compensation for Impact-Based Grain Flow Sensor. In: Li D., Chen

688 Y. (eds) *Computer and Computing Technologies in Agriculture V. CCTA 2011. IFIP Advances in*

689 *Information and Communication Technology*, vol 370, 210-216, Berlin, Heidelberg, Germany: Springer

690 Hubert, M., & Van der Veecken, S. (2008). Outlier detection for skewed data. *Journal of Chemometrics*, 22, 235-

691 246

692 Jingtiao, Q., & Shuhui, Z. (2010). Experiment research of impact-based sensor to monitor corn ear yield.

693 *International Conference on Computer Application and System Modeling*, IEEE, 101, 187-192.

694 Lee, D. H., Sudduth, K. A., Drummond, S. T., Chung, S. O., & Myers, D. B. (2012). Automated yield map delay

695 identification using phase correlation methodology. *Transactions of the ASABE* 55, 743-752.

696 Leroux, C., Jones, H., Clenet, A., Dreux, B., Becu, M., Tisseyre, B. (2017). Simulating yield datasets: an

697 opportunity to improve data filtering algorithms. In J A Taylor, D Cammarano, A Preashar, A Hamilton

698 (Eds.), *Proceedings of the 11<sup>th</sup> European Conference on Precision Agriculture*, Precision Agriculture '17

699 (*Advances in Animal Biosciences* 8 (2) 600-605).

700 Lu, C-T., Chen, D., & Kou, Y. (2003). Algorithms for spatial outlier detection. In X.Wu, A. Tuzhilin, and J.

701 Shavlik (Eds.) *Proceedings of the Third IEEE International Conference on Data Mining*, Los Alamitos, CA,

702 USA: IEEE Press, pp 597-600.

703 Lyle, G., Bryan, B., & Ostendorf, B. (2013). Post-processing methods to eliminate erroneous grain yield

704 measurements: review and directions for future development. *Precision Agriculture*, 15, 377-402.

705 Pringle, M. J., McBratney, A. B., Whelan, B. M., & Taylor, J. A. (2003). A preliminary approach to assessing the

706 opportunity for site-specific crop management in a field, using a yield monitor. *Agricultural Systems*, 76,

707 273-292.

708 R Core Team (2013). R: A language and environment for statistical computing. *R Foundation for Statistical*

709 *Computing*, Vienna, Austria.

710 Reinke, R., Dankowicz, H., Phelan, J., & Kang, W. (2011). A dynamic grain flow model for a mass flow yield

711 sensor on a combine. *Precision Agriculture*, 12, 732-749

712 Reitz, P., & H. D. Kutzbach (1996). Investigations on a particular yield mapping system for combine harvesters.

713 *Computers and Electronics in Agriculture*, 14, 137-150.

714 Robinson, T. P., & Metternicht, G. (2005). Comparing the performance of techniques to improve the quality of

715 yield maps. *Agricultural Systems*, 85, 19-41

716 Sawant, K. (2014). Adaptive methods for determining DBSCAN parameters. *International Journal of Innovative*

717 *Science, Engineering & Technology*, 1, 330-334

- 718 Simbahan, G.C., Dobermann, A., & Ping, J.L. (2004). Screening yield monitor data improves grain yield maps.  
719 *Agronomy Journal*, 96, 1091-1102
- 720 Spekken, M., Anselmi, A. A., & Molin, J. P. (2013). A simple method for filtering spatial data. In J.V. Stafford  
721 (Ed.), *Precision agriculture '13: Proceedings of the 9th European Conference on precision agriculture. The*  
722 *Netherlands: Wageningen Academic Publishers*, pp 259-266.
- 723 Sudduth, K., & Drummond, S. T. (2007). Yield Editor : Software for Removing Errors from Crop Yield Maps.  
724 *Agronomy Journal*, 99, 1471.
- 725 Sun, W., Whelan, B., McBratney, A.B., & Minasny, B. (2013). An integrated framework for software to provide  
726 yield data cleaning and estimation of an opportunity index for site-specific crop management. *Precision*  
727 *Agriculture*, 14, 376–391.
- 728 Taylor, J. A., Mcbratney, A. B., & Whelan, B. M. (2007). Establishing Management Classes for Broadacre  
729 Agricultural Production. *Agronomy Journal*, 99, 1366–1376.
- 730 Tobler W. (1970) A computer movie simulating urban growth in the Detroit region. *Economic Geography*, 46,  
731 234-240
- 732 Zhao, C., Huang, W., Chen, L., Meng, Z., Wang, Y., & Xu, F. (2010). A harvest area measurement system based  
733 on ultrasonic sensors and DGPS for yield map correction. *Precision Agriculture*, 11, 163-180.